**Author for correspondence:**
Roi Holzman
e-mail: holzman@post.tau.ac.il

# THE ROYAL SOCIETY
PUBLISHING

# Hydrodynamic regime determines the feeding success of larval fish through the modulation of strike kinematics

Victor China[1,3,†], Liraz Levy[1,3,†], Alex Liberzon[2], Tal Elmaliach[3] and Roi Holzman[1,3]

[1]Department of Zoology, Faculty of Life Sciences, and [2]School of Mechanical Engineering, Faculty of Engineering, Tel Aviv University, Tel Aviv 69978, Israel
[3]The Inter-University Institute for Marine Sciences, PO Box 469, Eilat 88103, Israel

AL, 0000-0002-6882-4191; RH, 0000-0002-2334-2551

Larval fishes experience extreme mortality rates, with 99% of a cohort perishing within days after starting to actively feed. While recent evidence suggests that hydrodynamic factors contribute to constraining larval feeding during early ontogeny, feeding is a complex process that involves numerous interacting behavioural and biomechanical components. How these components change throughout ontogeny and how they contribute to feeding remain unclear. Using 339 observations of larval feeding attempts, we quantified the effects of morphological and behavioural traits on feeding success of *Sparus aurata* larvae during early ontogeny. Feeding success was determined using high-speed videography, under both natural and increased water viscosity treatments. Successful strikes were characterized by Reynolds numbers that were an order of magnitude higher than those of failed strikes. The pattern of increasing strike success with increasing age was driven by the ontogeny of traits that facilitate the transition to higher Reynolds numbers. Hence, the physical growth of a larva plays an important role in its transition to a hydrodynamic regime of higher Reynolds numbers, in which suction feeding is more effective.

## 1. Introduction

Most pelagic and benthic marine fishes reproduce by external fertilization of eggs, which are then broadcast into the water column [1–3]. Larvae hatch from these pelagic eggs, and subsist on a yolk sac for several days until the mouth forms [4]. The period immediately after larvae initiate feeding is characterized by mass mortality within the cohort, reaching over 90% within the course of several days [5]. Starvation, resulting from the inability of larvae to find sufficient prey, was originally suggested as the key agent of mortality during this 'critical period' of mass mortality [5]. Predation, advection to unsuitable habitats and disease were also hypothesized to contribute to larval mortality during this period [1–3,6]. However, a 'critical period' of over 70% larval mortality is also commonly observed in mariculture facilities [7]. This high mortality, even under conditions of high concentrations of food, the absence of predators and controlled environmental conditions, implies that additional mechanisms may contribute to mortality during the critical period.

To capture their prey, larval fishes swim towards it and open their mouth while expanding their buccal cavity. This expansion generates a strong flow of water into the mouth, overcoming the escape responses of the prey and drawing it into the mouth [8–10]. Similarly to the effect of larval size on the hydrodynamics of their swimming [11], the characteristics of the suction flows that larvae generate change with size [10]. In general, the hydrodynamic regime characterizing the interaction of a fluid and a solid body (e.g. an organism) depends on the body's dimensions, the flow speed around it and fluid

properties (density and dynamic viscosity). The flow regime is commonly characterized by the dimensionless Reynolds number ($Re$):

$$Re = \frac{\rho \cdot l \cdot u}{\mu}, \tag{1.1}$$

where $\rho$ is the density of the fluid (kg m$^{-3}$), $l$ the characteristic length (m), $u$ the flow speed (m s$^{-1}$) and $\mu$ the dynamic viscosity (N s m$^{-2}$). As $Re$ increases, inertial forces become more dominant than viscous forces [12]. Consequently, there are hydrodynamic differences in the way larvae and adult fish experience their environment [9,13]. The flow regime affects larval swimming performance owing to its effect on the tendency of the fluid to separate from the fins, and the larval ability to impart momentum to the surrounding fluid [13]. Furthermore, while the effects of viscous forces on suction-feeding hydrodynamics in adult fish predominantly affect the flow inside the mouth cavity [14], these forces have a pronounced effect on the characteristics of suction flow outside the mouth in larval fish [10]. For example, when viscous forces dominate, the force required to accelerate the fluid increases [15] and spatial gradients in the suction flow exterior to the mouth become more gradual [10]. Note that different scales may apply for different flow fields around the organism. For example, the hydrodynamic regime that characterizes larval swimming ($Re_{(\text{swimming})}$) is defined using the larva's body length and swimming speed, whereas the hydrodynamic regime that characterizes its suction flow ($Re_{(\text{feeding})}$) is defined using gape diameter and the speed of the suction flow.

During ontogeny, fish larvae transition from a regime of low $Re$ at first feeding to a much higher $Re$ at later ages [8–10,13,16]. The $Re_{(\text{feeding})}$ for first-feeding larvae is approximately 20, while for individuals at the end of the larval period, $Re_{(\text{feeding})}$ is approximately 200 ($Re$ estimated based on a computation fluid dynamics model of suction feeding; [10]). This transition to high $Re_{(\text{feeding})}$ is accompanied by a steep increase in prey capture success and feeding rates [8,9,17,18]. Concomitantly, larvae undergo pronounced morphological and developmental changes. Immediately after the larvae hatch, a rapid restructuring of the moto-sensory system occurs [19]. As ontogeny progresses, the skeleton ossifies, muscle mass increases, the eyes grow and coordination improves. The developmental state of early-stage larvae prior to such changes has been hypothesized to impede their feeding [20–24]. Thus, two distinct mechanisms can affect feeding success throughout ontogeny: (i) changes in the hydrodynamic regime experienced by the larvae ($Re_{(\text{feeding})}$ and $Re_{(\text{swimming})}$, resulting from their increasing body length and gape diameter and their ability to generate faster swimming and suction flow speeds); and (ii) developmental and behavioural changes that do not affect the hydrodynamic environment (e.g. improved visual acuity).

Recently, it was suggested that hydrodynamic constraints on the ubiquitous suction-feeding mechanism of early-stage larvae lead to low feeding rates, even under high food concentrations [8–10]. As a way to alter the hydrodynamic regime in which the larvae dwell, independently of their development, those studies manipulated the viscosity ($\mu$ in equation (1.1)) of the medium inhabited by the larvae ('dynamic-scaling experiments'; [8,25]). The experiments were based on the principle that, when comparing two flow regimes imposed on an object (the larva), the two regimes will be hydrodynamically identical if the non-dimensional parameters ($Re$) are identical. It is thus possible to replicate the hydrodynamic regime experienced by a small larva (e.g. 3.5 mm in length) by submerging a larger larva (e.g. 7 mm) in a high-viscosity solution. When viscosity is increased in proportion to length (equation (1.1)) and assuming no change in speed, the two larvae share the same hydrodynamic environment but differ in their age, length, level of experience and many other morphological features that change throughout development. For example, the younger 3.5 mm larva will be characterized by a lower degree of bone ossification, poorer visual acuity, lesser prey-handling experience and an under-developed motor-neural system compared with an older (more developed) 7 mm larva [20–24]. Hereafter, we refer to phenotypic changes that are not associated with linear growth as 'developmental factors'. If these developmental factors are dominant in determining feeding success, then placing the older, more developed larva in a low $Re$ environment should have a relatively minor effect on its feeding success. Alternatively, if the hydrodynamic environment dictates feeding success, then placing the older, more developed larva in a low $Re$ environment should have a strong effect on its feeding success. This is because many parameters of the suction flow (e.g. its spatio-temporal pattern and the forces it exerts on the prey) are dependent on the hydrodynamic environment ($Re$), which is a function of size (increasing through ontogeny) and viscosity (which we increased experimentally). Previous dynamic-scaling experiments indicate a strong effect of the hydrodynamic environment on larval feeding. For example, larval feeding rates were determined by the dynamically scaled size of the larvae, while no significant effect of age on feeding rates was observed [8]. Additional modelling [10] indicated that the spatial patterns of the suction flows change as a function of $Re$, such that a low $Re$ environment impedes the force exerted on the prey and restricts the distance from which it can be captured.

Suction feeding is a complex behaviour, composed of multiple morpho-physiological traits (hereafter 'm-p traits'; [26]). These include the size of the mouth, the speed of mouth opening and the distance to the prey at the initiation of feeding strike [8,10,26], all of which combine to determine the outcome of the predator–prey interaction. In the context of larval feeding, it is not known how these m-p traits interact to contribute to feeding performance throughout ontogeny. The goals of this study were twofold: first, to examine the role of the hydrodynamic environment in determining the outcome of prey-acquisition strikes (success or failure) in larval fish; and second, to quantify the effect of major m-p traits on the hydrodynamic regime that characterizes these strikes. We analysed 339 feeding interactions and compared the hydrodynamic regime and the m-p trait values for failed and successful strikes throughout larval ontogeny. In addition, we adjusted water viscosity to manipulate the hydrodynamic regime independently of other developmental factors.

## 2. Methods

### (a) Experimental approach

We used two separate high-speed video systems to test each of our two hypotheses. To examine whether the hydrodynamic environment determines the outcome of prey-acquisition strikes, we used a three-dimensional high-speed camera system,
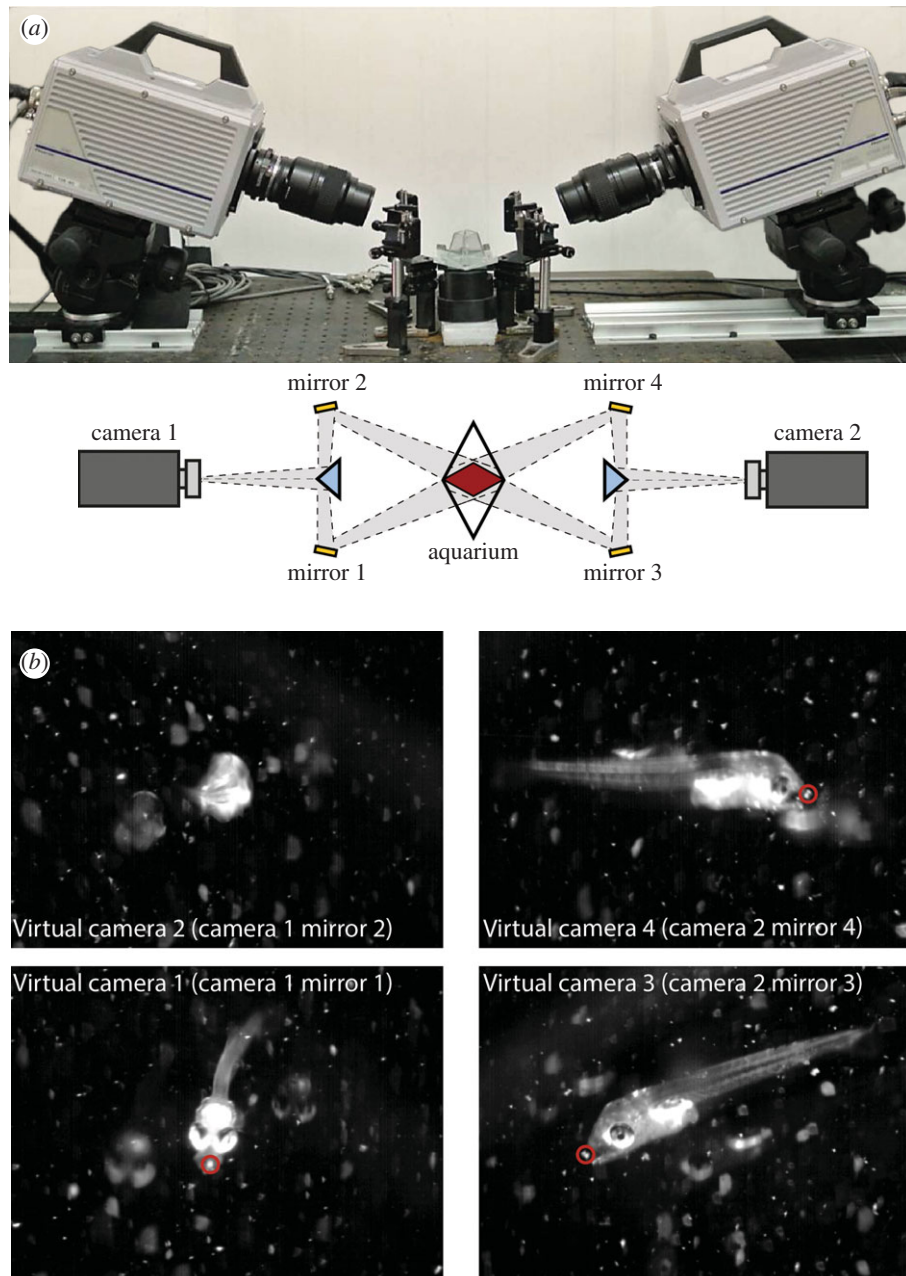
**Figure 1.** The three-dimensional high-speed filming system. (*a*) Side and top views of the three-dimensional set-up (photo and schematic, respectively) showing the positions of the cameras, mirror system and aquarium. Schematic top view is not to scale. Grey shading represents the camera viewing angles; red rhombus represents the regions of overlapping views (the 'visualized volume'). Orange rectangles and blue triangles represent the mirrors and beam splitters, respectively. (*b*) The set-up provides four perspectives of the fish within the visualized volume and permits three-dimensional tracking of landmarks on the fish and prey (denoted by a red circle). (Online version in colour.)

permitting accurate characterization of strike kinematics at 500 frames s$^{-1}$ (fps; see electronic supplementary material, '3D filming of prey acquisition strikes'; figure 1; movies S1–S3). The system was triggered manually, upon the observer's detection of a feeding strike, and recorded approximately 85 short video sequences (approximately 4 s) that typically included 1–2 strikes. To quantify the effect of m-p traits on the hydrodynamic regime that characterizes these strikes, we used a 250 fps continuous recording camera system. This system recorded long (approximately 8 min) high-speed videos, and feeding strikes were identified and categorized by reviewing the video at approximately 15 fps (see electronic supplementary material, 'Continuous high-speed system' [27]; movie S4). The fact that all the feeding events were recorded, regardless of their kinematics, resulted in a dataset that is unbiased with respect to the observers' ability to detect the strike in real time.

Using the three-dimensional system, we filmed *Sparus aurata* larvae ranging in age from 9 to 23 days post hatching (DPH) in

increments of 1–2 days (2–16 events for each age); using the continuous system, we filmed larvae aged 8, 13, 17 and 23 DPH (see electronic supplementary material, tables S1–S3). Fish were filmed feeding on rotifers (see electronic supplementary material, 'Study organisms').

## (b) Dynamic scaling experiments

We examined how changing the hydrodynamic environment of the larvae in each age group (8, 13, 17 and 23 DPH) affected feeding performance by manipulating the viscosity of the medium [8,25,28]. This allowed us to directly quantify the effects of the hydrodynamic regime (*Re* regime) which could be manipulated independently of other age-dependent developmental factors. We posited two possible factors that could influence larval feeding behaviour: (i) the hydrodynamic environment and (ii) the experience and ability of the larva given its developmental state. If strike characteristics are mainly dictated by the hydrodynamic
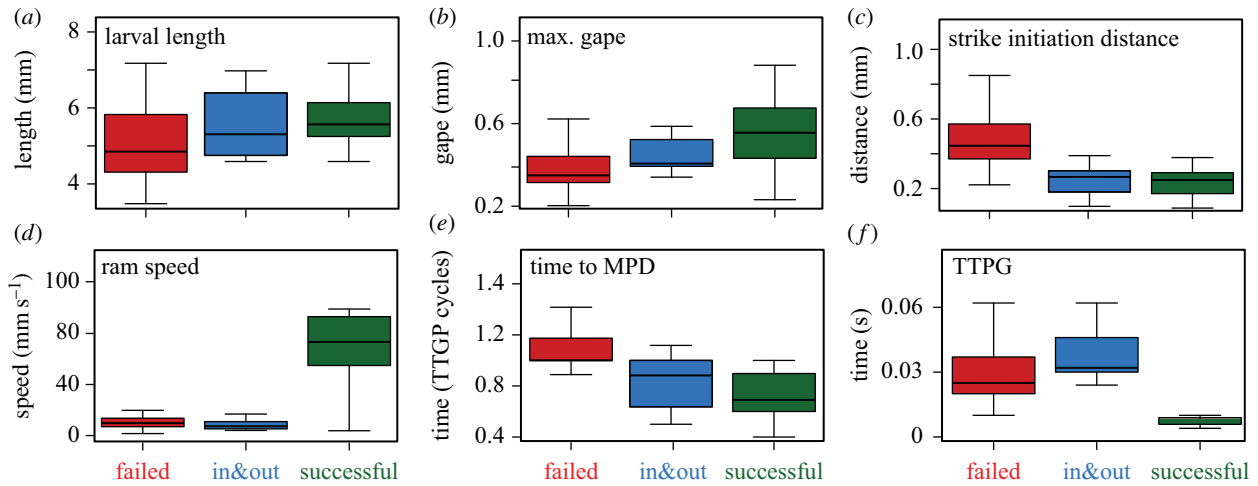
**Figure 2.** Strike outcomes and their kinematics: kinematics of 'failed' (red), 'in&out' (blue) and 'successful' (green) feeding attempts. Data were obtained with the three-dimensional high-speed system ($n = 93$ strikes; electronic supplementary material, table S2). For visualization purposes, data are pooled for all ages. Boxes encompass the range between first and third quartile, whiskers span 1.5 inter-quartile range; the horizontal line within each box is the median. MPD in (e) denotes minimal prey distance; TTPG in (f) is time to peak gape. (Online version in colour.)

environment, we expect older/larger larvae in experimentally manipulated viscous regime ('dynamically scaled larvae') to perform similarly to younger/smaller larvae in unmanipulated water regardless to their experience and developmental state. If strike characteristics are also dictated by the developmental state of the larvae, we expect 'dynamically scaled' larvae to show different strike characteristics from those of younger larvae in unmanipulated water. Viscosity was manipulated by dissolving increasing quantities of dextran in seawater. Each age group was filmed using the continuous high-speed system under three viscosities: unmanipulated seawater ($1.08 \times 10^{-3}$ Pa s); a solution of seawater and dextran with viscosity equivalent to $\times 1.4$ that of seawater (approx. $1.5 \times 10^{-3}$ Pa s); and a solution of seawater and dextran with viscosity equivalent to $\times 2.1$ that of seawater (approx. $2.27 \times 10^{-3}$ Pa s). In addition, the 23 DPH age group was filmed in a solution of approximately $2.9 \times 10^{-3}$ Pa s, equivalent to $2.7\times$ viscosity of seawater (see electronic supplementary material, 'optical properties of dextran solutions').

## (c) Data analysis

Feeding attempts were defined as instances in which mouth opening generated movement of the prey towards the mouth [9]. Attempts were classified as 'successful' if a food item entered and remained in the mouth during and after mouth closing. Failed strikes were categorized as 'failed' if the prey did not enter the mouth and as 'in&out' if prey entered the mouth but exited while the mouth was closing. For the three-dimensional high-speed camera system, only feeding attempts in which both the larva and the prey were viewed in focus by at least two virtual cameras were used, resulting in 93 analysed feeding attempts. For the continuous high-speed system, only feeding attempts in which the sagittal plane of the larva appeared perpendicular to the plane of the camera were used, resulting in 246 analysed feeding strikes (electronic supplementary material, tables S1–S3).

For each video (2–4 views in the three-dimensional system, one in the continuous system), we digitized five landmarks on the body, jaws and prey to calculate a set of nine variables: (i) larval length, (ii) buccal length (mm), (iii) maximal and minimal gape diameter (mm), (iv) time to peak gape (TTPG; ms), (v) average gape speed (mm s$^{-1}$), (vi) strike initiation distance (mm), (vii) swimming speed (ram; mm s$^{-1}$), (viii) time to minimal prey distance (time to MPD) and (ix) maximal flow speed at the gape aperture (hereafter 'peak flow speed'; mm s$^{-1}$). (See 'Measured variables' in electronic supplementary material.) We also calculated the Re for feeding and swimming: $Re_{(feeding)}$ was calculated using maximal gape diameter

as the relevant length ($l$ in equation (1.1)) and peak flow speed ($u$ in equation (1.1)). $Re_{(swimming)}$ was calculated using larval length as the relevant length ($l$ in equation (1.1)), and larval swimming speed ($u$ in equation (1.1)).

## (d) Statistical analysis

Discriminant function analysis (DFA) was used to determine how the hydrodynamic regime predicts strike outcome, using data obtained with our three-dimensional high-speed camera system (see electronic supplementary material for details). The grouping variable was strike outcome ('failed', 'in&out' or 'successful') and the independent variables were $Re_{(feeding)}$, $Re_{(swimming)}$, time to MPD and strike initiation distance. These independent variables took into account all m-p traits that we measured because TTPG, peak flow speed, maximal gape size, swimming speed and larval length were used to calculate $Re_{(feeding)}$ and $Re_{(swimming)}$. Discriminant function produces a table of structure scores that estimate the contribution of each variable to separating the classified events and a confusion matrix, which reveals the number of cases that are misclassified in the pre-determined groups.

We used path analysis (see electronic supplementary material for details) to test two complementary questions: (1) how do larval size and age affect the hydrodynamic regime in which the larvae swim and feed; and, consequently, how does the hydrodynamic regime determine feeding success? and (2) how do size and viscosity affect feeding success through their direct effects on each m-p trait within the feeding mechanism? Our first model (question 1) included larval age and size as independent continuous variables, $Re_{(feeding)}$ and $Re_{(swimming)}$ as dependent continuous variables, and strike outcome as a dependent categorical variable. The second model (question 2) comprised larval age, larval length and viscosity as independent continuous variables; TTPG, gape speed, time to MPD, strike initiation distance, swimming speed, peak flow speed and gape length as dependent continuous variables; and strike outcome as a dependent categorical variable (figure 2).

# 3. Results

## (a) Strike outcome is determined by $Re_{(feeding)}$

Evaluation of morphological and kinematic traits obtained with our three-dimensional high-speed camera system revealed differences between the three strike outcomes
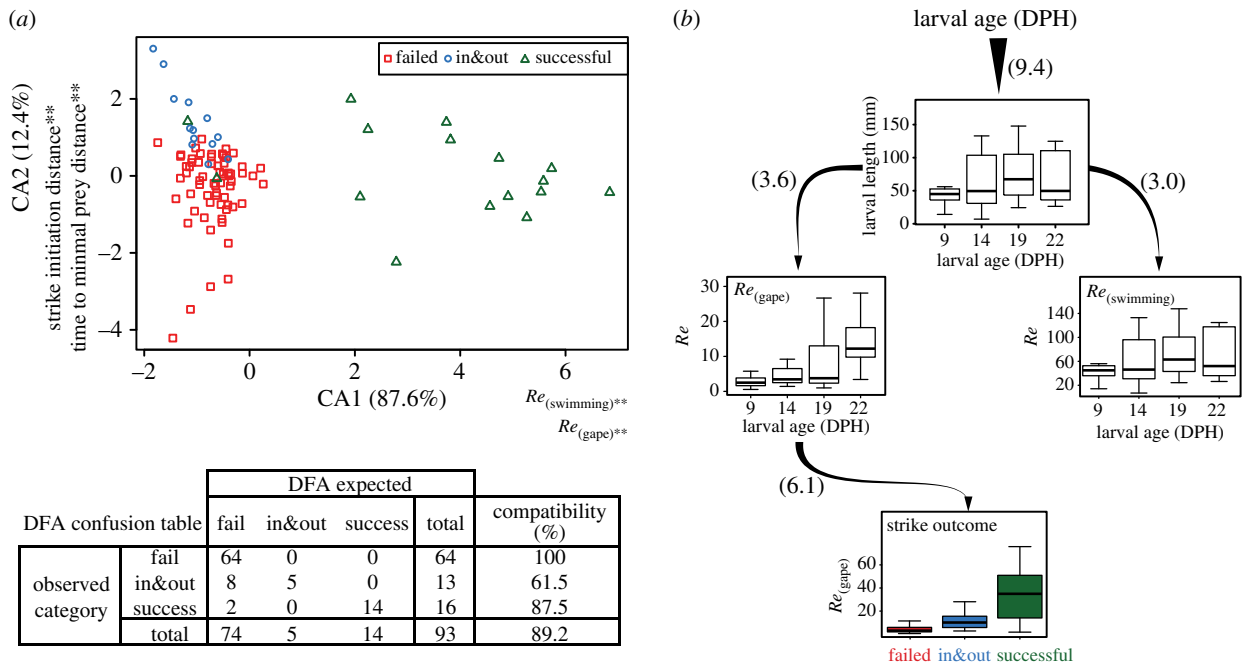
**Figure 3.** The effect of the hydrodynamic regime on feeding success throughout the critical period of *Sparus aurata* larvae. (*a*) DFA indicates that the separation between successful strikes and the two failure categories ('failed', 'in&out') was driven by $Re_{(feeding)}$ and $Re_{(swimming)}$ (first canonical axis; CA1), whereas the separation between 'failed' and 'in&out' events was driven by strike initiation distance and the time to minimal prey distance (CA2). Confusion table details the percentage of correctly classified events. (*b*) Path analysis was used to quantify the direct (indicated by arrows) and indirect effects of the hydrodynamic environment on feeding success. Binning data by age groups was done for visualization purposes only. Boxes encompass the range between first and third quartile, whiskers span 1.5 inter-quartile range; the horizontal line within each box is the median. Data in (*a*) and (*b*) obtained with the three-dimensional system. (Online version in colour.)

(figure 2; electronic supplementary material, figure S1 and movies S1–S3). Larvae that managed to successfully capture their prey were larger in size (mean standard length = 5.59 versus 5.10 mm, respectively; figure 2*a*), and their average gape diameter was ×1.5 larger than that appearing in failed strikes (mean gape = 0.56 mm versus 0.39 mm, respectively; figure 2*b*). In addition, successful strikes were characterized by fast kinematics. Ram speed was sevenfold faster (mean ram = 71.4 versus 10.6 mm s$^{-1}$, respectively; figure 2*d*) and average TTPG was shorter by 50% (mean TTPG = 0.012 versus 0.03 s, respectively; figure 2*f*) than for unsuccessful strikes. Even though the kinematics of in&out strikes were generally similar to those of successful ones, in&out strikes were characterized by much longer TTPGs and slower ram speeds than successful strikes (figure 2; electronic supplementary material, figure S1), resulting in a failure to retain the prey in the mouth before it closed.

To understand how variation in m-p traits affects the hydrodynamic regime in which the larvae forage, we performed a DFA of the hydrodynamic characteristics of feeding attempts, using $Re_{(feeding)}$, $Re_{(swimming)}$, strike initiation distance and time to MPD. This analysis provided a high degree of separation between the different strike outcomes, with 89.2% correct classification (figure 3*a*; $p < 0.001$). Specifically, failed attempts were always correctly classified (100% correct classification), successful attempts were correctly classified 87.5% of the time, while in&out attempts were often (61.5%) classified as 'failed' but never as successful strikes (see confusion table in figure 3*a*). The first canonical axis produced by the DFA accounted for approximately 88% of the variance explained (figure 3*a*), and separated successful strikes from the two other unsuccessful categories ('failed' and 'in&out'). On this axis, the hydrodynamic characteristics of the strike ($Re_{(feeding)}$ and $Re_{(swimming)}$) were the strongest

predictors of strike outcome with structure score of 0.94 and 0.95, respectively, indicating a 'strong' effect on strike outcome. The second canonical axis separated between the unsuccessful categories ('failed' and 'in&out'). On this axis, strike initiation distance and time to MPD had 'strong' effects ($-0.72$ and $0.65$, respectively; electronic supplementary material, table S4).

Path analysis models of feeding attempts constructed for both datasets (three-dimensional and continuous high-speed camera systems) produced very similar outcomes (electronic supplementary material, table S5). In both cases, larval age and length affected strike outcome exclusively through their effect on strike hydrodynamics ($Re_{(feeding)}$; figure 3*b*). Larval age positively affected larval length, which in turn positively affected both $Re_{(feeding)}$ and $Re_{(swimming)}$. Strike outcome was directly affected only by $Re_{(feeding)}$, whereas larval age and length affected strike outcome via their direct or indirect effect on $Re_{(feeding)}$. $Re_{(swimming)}$ had no significant direct or indirect effect on strike outcome (figure 3*b*; electronic supplementary material, table S5). Note that for strikes recorded with the three-dimensional system, variability in $Re$ between strikes was driven by intrinsic factors such as larval body and gape size, and swimming and suction speed, whereas for strikes recorded with the continuous system, $Re$ was also experimentally manipulated by increasing the viscosity of the medium in which the larvae foraged.

## (b) Size and viscosity had opposite effects on strike kinematics

We used a second path analysis model to account for the complex and indirect ways in which m-p traits may interact to determine strike outcome. Here, we used all m-p traits measured for each strike, visualized with our continuous
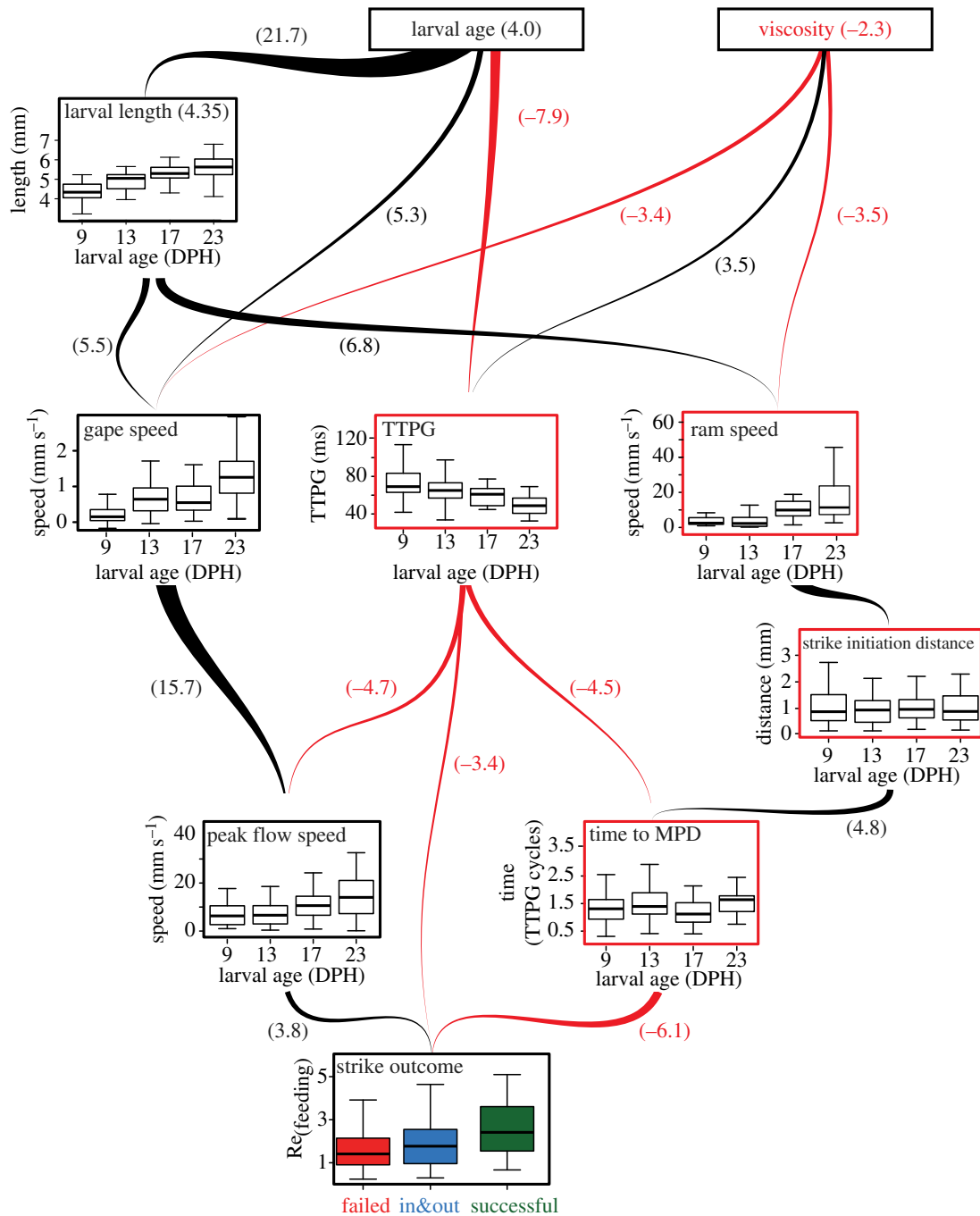
**Figure 4.** Path analysis indicates strike success is mediated through multiple interacting m-p traits. Black and red arrows represent statistically significant positive and negative paths, respectively. Red and black panel frames represent positive and negative total effects of each variable on strike outcome. The effect size of each path (arrow) is denoted by the bracketed values and arrow width (see electronic supplementary material, tables S5 – S7). Strike outcome was directly determined by peak flow speed, TTPG and time to MPD. Increasing larval age/length decreased TTPG and increased ram and gape speeds, while viscosity had opposite effects on these variables. Total effect sizes (the sum of all direct and indirect paths) of larval age, length and viscosity are denoted near variable names. Boxes encompass the range between first and third quartile, whiskers span 1.5 inter-quartile range; the horizontal line within the box is the median. (Online version in colour.)

system, as well as larval age, and the viscosity of the medium in which the larvae foraged. This analysis revealed direct paths (i.e. direct effects) from peak flow speed, time to MPD and TTPG to strike outcome. Strike initiation distance, ram speed, gape speed, larval length, larval age and viscosity affected feeding success only indirectly, through their effects on other variables (i.e. no significant direct paths to strike outcome). TTPG had both direct and indirect effects on strike outcome (figure 4; electronic supplementary material, table S6). The total effect of larval age on feeding success was positive, whereas ram speed and TTPG had negative total effects on feeding success. Viscosity had contrasting effects to those of ontogeny (larval size and age); with effect

sizes that were similar in absolute magnitudes but with opposite signs on TTPG, gape opening speed and ram speed (figure 4; electronic supplementary material, table S6). The total effect of age (the sum of all direct and indirect effects) on feeding success was 4.0, while the total effect of viscosity was −2.3, indicating a pattern of increasing feeding success with increasing age and decreasing viscosity ($p < 0.001$ and $p < 0.002$, respectively).

It is possible that the mechanical feedback undergoes change if the viscosity of the seawater is increased, causing the fish to use suboptimal motor patterns that yield suboptimal performance. However, the lack of a direct effect of viscosity on strike outcome suggests that our experimental

manipulation of the fluid viscosity did not bias the larval feeding behaviour, and that such effects were weak.

## 4. Discussion

Our results indicate that the success of a strike is determined by its hydrodynamic characteristics: successful strikes were characterized by an $Re_{(feeding)}$ that was an order of magnitude higher than that of failed strikes (figure 3). Our path analysis revealed that the effects of size and age on strike success are mediated through their effects on $Re_{(feeding)}$, with no significant direct paths from either size or age to strike outcome (figure 3b). Thus, only individual larvae that manage to momentarily escape the viscous low $Re$ regime during their prey acquisition strike are able to capture their prey. We suggest that the ontogenetic pattern of increasing strike success within the age range we studied is largely driven by the ontogeny of traits that facilitate the transition to higher $Re$.

Our path analysis indicates that the effect of larval size on the different m-p traits is directly related to hydrodynamics: older larvae operate in higher $Re$ because they are longer, have larger gape ($l$ in equation (1.1)) and shorter TTPG. Shorter TTPG and larger buccal volume resulted in faster suction flow and probably in steeper spatio-temporal gradients in front of the mouth [10]. Consequently, larvae feeding at higher $Re$ can exert stronger forces on their prey and, correspondingly, demonstrate greater feeding success. Larvae can further increase the force exerted on the prey by positioning it as close as possible to the mouth centre, where the pressure gradient is steepest and the flow speed is fastest [10,29]. This is reflected in the path analysis (figure 4), where the total effect of strike initiation distance on strike outcome is negative (shorter distance = higher prey capture probability). While the mechanism driving the 'in&out' events remains unclear, they are associated with low $Re_{(feeding)}$ and $Re_{(swimming)}$, although not as low as the 'failed' events (figure 3b). Recently, a particle image velocimetry study reported flow reversals in larval zebrafish, occurring frequently in smaller larvae towards the end of the gape cycle, when the mouth starts closing [30]. This could indicate that timing plays a more important role in determining strike outcome in larval fish than in adult fish, in which flow reversals are rare and minor [31].

Is feeding performance throughout the critical period affected by larval age primarily via its effect on the hydrodynamic regime experienced by the larvae? Previous research has suggested that feeding success of larval fishes improves with age due to ontogenetic improvement in the sensory system, coordination and experience. Such effects should have been manifested in our experiments in a significant path between age (or length) and strike outcome; however, our path analysis revealed that these expected relationships are non-significant. This conclusion is supported by the 'dynamic-scaling' experiments, specifically designed to tease apart the hydrodynamic effect of larval growth from other developmental factors. By increasing the viscosity of the medium in which the larvae foraged, we were able to expose older, larger larvae to the hydrodynamic regime that is typical of that experienced by younger, smaller larvae. However, a direct path between age and feeding success was not significant in our data, implying that the developmental factors play a relatively weak role in directly affecting strike outcome (in the age range we tested). The weak effect of developmental factors on strike outcome is further supported by the contrasting effects of larval age/length and viscosity in our model (figure 4). Artificially increasing the viscosity was associated with longer TTPG, slower ram speed and slower gape opening speed, resulting in a negative total effect on feeding success, while increasing larval age/length had opposite effects on these same variables. These contrasting effects can be expected if strike outcome is similarly affected by larval size and fluid viscosity, which change $Re$ in similar magnitude (but opposite directions). However, while developmental factors were found to be insignificant in our statistical analysis, they can potentially be important at earlier ages. Lankheet et al. [19] pointed out that a rapid, dramatic restructuring of the neuro-sensory system is important in determining feeding behaviour during the first day of feeding in precocial live-bearing fish. This may imply that during the first day(s) of active exogenous feeding (approximately 5 DPH in our study system), developmental factors may predominate in determining feeding behaviour in altricial, egg-hatched larvae.

The ability of larger larvae to feed in higher $Re$ can extend the range of prey types available to them. Consequently, the realized density of available prey is higher for larger larvae than for smaller ones: larger larvae can capture faster escaping prey, and exert sufficient force to suck heavier (denser) prey into their mouth. This higher realized prey density also augments the encounter rate with prey, defined as the number of prey items entering the 'reactive volume' of the larvae within a given time frame. Therefore, encounter rate is also expected to increase with increasing swimming speed and with the distance at which the predator responds to the prey [32–34], both increasing through ontogeny (figure 4). The broader range of prey types and sizes, together with the longer feeding distance and faster swimming speeds realized by larger larvae, effectively increase the available food concentration, encounter rates and feeding opportunities. Ultimately, these are expected to increase feeding rates, a key factor in determining larval survival. Our findings that larger larvae feed better could also be relevant to the mariculture industry. We suggest that selecting for larger larval size at hatching or for yolk sacs with higher nutritional value could facilitate an improvement in batch survival and larval growth rates, as it may facilitate the escape from the low $Re$ regime experienced during initiation of exogenic feeding [13]. Additionally, our results indicate that direct observations on feeding events, performed for various prey types throughout larval ontogeny, could improve our understanding of feeding efficiency and help optimize larval diet. We note that focusing on the physical size and the escape response of the prey could further help match prey characteristics to larval feeding ability [35].

# References

1. Houde ED. 1987 Fish early life dynamics and recruitment variability. *Am. Fish. Soc. Symp.* **2**, 17–29.

2. Houde ED. 2008 Emerging from Hjort's shadow. *J. Northwest Atl. Fish. Sci.* **41**, 53–70. (doi:10.2960/J.v41.m634)

3. Houde ED. 1989 Comparative growth, mortality, and energetics of marine fish larvae: temperature and implied latitudinal effects. *Fish. Bull.* **87**, 471–495.

4. Pauly D, Pullin RV. 1988 Hatching time in spherical, pelagic, marine fish eggs in response to temperature and egg size. *Environ. Biol. Fishes* **22**, 261–271. (doi:10.1007/BF00004892)

5. Hjort J. 1914 Fluctuations in the great fisheries of northern Europe. *Rapp. P.-v. Réun. Cons. Perm. Int. Explor. Mer* **20**, 1–28.

6. Cowen RK, Sponaugle S. 2009 Larval dispersal and marine population connectivity. *Ann. Rev. Mar. Sci.* **1**, 443–466. (doi:10.1146/annurev.marine.010908.163757)

7. Shields RJ. 2001 Larviculture of marine finfish in Europe. *Aquaculture* **200**, 55–88. (doi:10.1016/S0044-8486(01)00694-9)

8. China V, Holzman R. 2014 Hydrodynamic starvation in first-feeding larval fishes. *Proc. Natl Acad. Sci. USA* **111**, 8083–8088. (doi:10.1073/pnas.1323205111)

9. Holzman R, China V, Yaniv S, Zilka M. 2015 Hydrodynamic constraints of suction feeding in low Reynolds numbers, and the critical period of larval fishes. *Integr. Comp. Biol.* **55**, 48–61. (doi:10.1093/icb/icv030)

10. Yaniv S, Elad D, Holzman R. 2014 Suction feeding across fish life stages: flow dynamics from larvae to adults and implications for prey capture. *J. Exp. Biol.* **217**, 3748–3757. (doi:10.1242/jeb.104331)

11. Muller UK, van den Boogaart JGM, van Leeuwen JL. 2008 Flow patterns of larval fish: undulatory swimming in the intermediate flow regime. *J. Exp. Biol.* **211**, 196–205. (doi:10.1242/jeb.005629)

12. Vogel S. 1994 *Life in moving fluids: the physical biology of flow*. Princeton, NJ: Princeton University Press.

13. Müller UK, Videler JJ. 1996 Inertia as a 'safe harbour': do fish larvae increase length growth to escape viscous drag? *Rev. Fish Biol. Fish.* **6**, 353–360. (doi:10.1007/BF00122586)

14. Van Wassenbergh S, Aerts P. 2009 Aquatic suction feeding dynamics: insights from computational modelling. *J. R. Soc. Interface* **6**, 149–158. (doi:10.1098/rsif.2008.0311)

15. Drost MR, Muller M, Osse JWM. 1988 A quantitative hydrodynamical model of suction feeding in larval fishes—the role of frictional forces. *Proc. R. Soc. Lond. B* **234**, 263–281. (doi:10.1098/rspb.1988.0048)

16. Osse JWM, Boogaart JGM. 1999 Dynamic morphology of fish larvae, structural implications of friction forces in swimming, feeding and ventilation. *J. Fish Biol.* **55**, 156–174. (doi:10.1111/j.1095-8649.1999.tb01053.x)

17. Drost MR. 1987 Relation between aiming and catch success in larval fishes. *Can. J. Fish. Aquat. Sci.* **44**, 304–315. (doi:10.1139/f87-039)

18. Blaxter JHS. 1980 Vision and feeding of fishes. In *Fish behaviour and its use in the capture and culture of fishes* (eds Bardach JE, Magnuson JJ, May RC, Reinhart JM). Iclarm Conference Proceedings no. 5, pp. 32–56. Manila, Philippines: International Center for Living Aquatic Resources Management Manila.

19. Lankheet MJ, Stoffers T, van Leeuwen JL, Pollux BJA. 2016 Acquired versus innate prey capturing skills in super-precocial live-bearing fish. *Proc. R. Soc. B* **283**, 20160972. (doi:10.1098/rspb.2016.0972)

20. Hubbs C, Blaxter JHS. 1986 Ninth Larval Fish Conference. Development of sense organs and behaviour of teleost larvae with special reference to feeding and predator avoidance. *Trans. Am. Fish. Soc.* **115**, 98–114. (doi:10.1577/1548-8659(1986)115<98:NLFCDO>2.0.CO;2)

21. Yúfera M, Darias MJ. 2007 The onset of exogenous feeding in marine fish larvae. *Aquaculture* **268**, 53–63. (doi:10.1016/j.aquaculture.2007.04.050)

22. Hunter JR. 1980 The feeding behavior and ecology of marine fish larvae. In *Fish behavior and its use in the capture and culture of fishes* (eds Bardach JE, Magnuson JJ, May RC, Reinhart JM). Iclarm Conference Proceedings no. 5, pp. 287–330. Manila, Philippines: International Center for Living Aquatic Resources Management.

23. Hunter JP. 1981 Feeding ecology and predation of marine fish larvae. In *Marine fish larvae: morphology, ecology, and relation to fisheries* (ed. R Lasker), pp. 33–77. Seattle, WA: University of Washington Press.

24. Budick SA, O'Malley DM. 2000 Locomotor repertoire of the larval zebrafish: swimming, turning and prey capture. *J. Exp. Biol.* **203**, 2565–2579.

25. Danos N, Lauder GV. 2012 Challenging zebrafish escape responses by increasing water viscosity. *J. Exp. Biol.* **215**, 1854–1862. (doi:10.1242/jeb.068957)

26. Holzman R, Collar DC, Mehta RS, Wainwright PC. 2012 An integrative modeling approach to elucidate suction-feeding performance. *J. Exp. Biol.* **215**, 1–13. (doi:10.1242/jeb.057851)

27. Shamur E, Zilka M, Hassner T, China V, Liberzon A, Holzman R. 2016 Automated detection of feeding strikes by larval fish using continuous high-speed digital video: a novel method to extract quantitative data from fast, sparse kinematic events. *J. Exp. Biol.* **219**, 1608–1617. (doi:10.1242/jeb.133751)

28. Bolton TF, Havenhand JN. 2005 Physiological acclimation to decreased water temperature and the relative importance of water viscosity in determining the feeding performance of larvae of a serpulid polychaete. *J. Plankton Res.* **27**, 875–879. (doi:10.1093/plankt/fbi060)

29. Holzman R, Day SW, Wainwright PC. 2007 Timing is everything: coordination of strike kinematics affects the force exerted by suction feeding fish on attached prey. *J. Exp. Biol.* **210**, 3328–3336. (doi:10.1242/jeb.008292)

30. Pekkan K, Chang B, Uslu F, Mani K, Chen C-Y, Holzman R. 2016 Characterization of zebrafish larvae suction feeding flow using μPIV and optical coherence tomography. *Exp. Fluids* **57**, 95. (doi:10.1007/s00348-016-2197-6)

31. Day SW, Higham TE, Holzman R, Van Wassenbergh S. 2015 Morphology, kinematics, and dynamics: the mechanics of suction feeding in fishes. *Integr. Comp. Biol.* **55**, 21–35. (doi:10.1093/icb/icv032)

32. Kiørboe T, Saiz E. 1995 Planktivorous feeding in calm and turbulent environments, with emphasis on copepods. *Mar. Ecol. Ser.* **122**, 135–145. (doi:10.3354/meps122135)

33. MacKenzie BR, Kiørboe T. 1995 Encounter rates and swimming behavior of pause-travel and cruise larval fish predators in calm and turbulent laboratory environments. *Limnol. Oceanogr.* **40**, 1278–1289. (doi:10.4319/lo.1995.40.7.1278)

34. Viitasalo M, Kiorboe T, Flinkman J, Pedersen LW, Visser AW. 1998 Predation vulnerability of planktonic copepods: consequences of predator foraging strategies and prey sensory abilities. *Mar. Ecol. Ser.* **175**, 129–142. (doi:10.3354/meps175129)

35. Jackson JM, Lenz PH. 2016 Predator–prey interactions in the plankton: larval fish feeding on evasive copepods. *Sci. Rep.* **6**, 33585. (doi:10.1038/srep33585)

36. China V, Levy L, Liberzon A, Elmaliach T, Holzman R. 2017 Data from: Hydrodynamic regime determines the feeding success of larval fish through the modulation of strike kinematics. Dryad Digital Repository. (http://dx.doi.org/10.5061/dryad.s79j7)